

**ADDIS ABABA UNIVERSITY
SCHOOL OF GRADUATE STUDIES
DEPARTMENT OF CHEMISTRY**



Graduate Project (Chem.774)

**Study of EC mechanism by cyclic voltammetry:
Electrochemical oxidation of catechol in the presence of
imidazole**

By

Asfaw Negash

Advisor: Prof. Theodoros Solomon

**In Partial Fulfillment of the Requirements for Master of
Science Degree in Chemistry**

June, 2010

**ADDIS ABABA UNIVERSITY
SCHOOL OF GRADUATE STUDIES
DEPARTMENT OF CHEMISTRY**

Graduate Project (Chem.774)

**Study of EC mechanism by cyclic voltammetry: Electrochemical
oxidation of catechol in the Presence of imidazole**

Submitted by:

signature

Asfaw Negash

Approved by the examining Board:

signature

Prof. Theodros Solomon

Advisor

Prof. Teketel Yohannes

Examiner

Dr. Shimelis Admassie

Examiner

Declaration

I the undersigned confirm that the results reported in this work were obtained by research carried out by me under the supervision of my advisor in the Faculty of Science, Department of Chemistry, Addis Ababa University in the academic year 2009/2010.

Name _____

signature _____

This project work has been submitted for examination with my approval as University advisor.

Prof. Theodoros Solomon

signature _____

Submitted to:

School of Graduate Studies

Addis Ababa University

Acknowledgement

First and foremost I offer my deepest heart-felt thanks and glory to my Almighty God, who is the source of my strength and inspiration in the ups and downs of my life. I believe that he is the God who opened the door of education to me and who helped and gave me success in all ways.

I am deeply indebted to prof. Theodros Solomon for his invaluable guidance, genuine concern to in any aspect, unreserved support, constant encouragement, sitting for longer hours of discussions and consultations, and comments on the work through out the study.

My thanks go to my wife Hareg Yeshitila and my sister Mimi Negash for their material support and never ending moral encouragement. I would like thank my friends Belete Tesfaw and Yitina Gebre for their friendly co-operation, support and advice in various ways.

Finally, I would like thank to Addis Ababa Education Bureau allowing me to continue my education and providing sponsorship.

Table of content	page
Acknowledgement-----	i
List of figure-----	iii
List of scheme-----	v
List of table-----	v
Abstract -----	vi
1. Introduction-----	1
1.1. Coupled Chemical Reaction -----	1
1.2. Literature review-----	3
1.3. Objectives of the study -----	8
2. Characterization of chemical reactions coupled with electron transfer by cyclic voltammetry-----	9
2.1. Basics of cyclic voltammetry-----	9
2.2. EC mechanism-----	12
2.3. Diagnostic test-----	17
3. Experimental part -----	17
3.1. Reagents and chemicals-----	17
3.2. Instrumentation-----	17
3.3. Electrolytic cells and electrodes-----	17
3.4. Procedure-----	17
4. Result and discussion-----	19
4.1. Electrochemical investigations of catechol-----	19
4.2. Electrochemical investigation of catechol in the Presence of imidazole -----	22
4.3. Effect of pH-----	23
4.4. Effect of scan rate-----	26
4.5. Mechanism-----	31
4.6. Kinetics study-----	32
5. Conclusion-----	34
6. References-----	35

List of figure	page
Figure. 1 Steps constituting a typical organic electrode reaction-----	2
Figure .2 a) Excitation waveform and b) response obtained for the reversible by cyclic Voltammetry-----	10
Figure 3. Cyclic voltammograms for E_rC_i case at 25°C-----	13
Figure 4. Ratio of anodic to cathodic peak current as a function of $k_f \tau$, where τ is the time between $E_{1/2}$ and the switching potential E_λ -----	14
Figure 5. Variation of peak potential as a function of λ for the E_rC_i case-----	15
Figure 6. Typical voltammograms of 1.0 mM catechol at the glassy carbon electrode, in 0.2 M phosphate buffer of pH 7.0 at scan rates 25, 50, 100,150, 200,250mV s ⁻¹ -----	19
Figure 7. Variation of I_p versus square root of scan rate ($v^{1/2}$) in electrochemical oxidation of 1.0mM catechol at a glassy carbon electrode in aqueous solution containing 0.2 M phosphate buffer of pH 7.0-----	20
Figure 8. Variation of ΔE_p versus scan rate in electrochemical oxidation of 1.0mM catechol at a glassy carbon electrode in aqueous solution containing 0.2 M phosphate buffer of pH 7.0-----	21
Figure 9. Variation of E_{pc} versus scan rate in electrochemical oxidation of 1.0 mM catechol at a glassy carbon electrode in aqueous solution containing 0.2 M phosphate buffer of pH 7.0-----	21
Figure 10. Cyclic voltammograms of 1.0 mM catechol in the absence (3) and presence of 1.67 mM imidazole (2), and that of a 1.0 mM 2 in the absence of catechol (1) at the glassy carbon electrode in 0.2 M aqueous phosphate buffer of pH 7.0 at a scan rate of 100 mV s ⁻¹ -----	23
Figure 11. Cyclic voltammograms of 1.0 mM catechol in the presence of 1.67 mM imidazole glassy carbon electrode at a scan rate of 100mVs ⁻¹ and various pH: (a) 4, (b) 5, (c) 6, (d)7, (e) 8-----	24
Figure 12. Variation of peak current ratio (I_{pc}/I_{pa}) versus pH in electrochemical oxidation of 1.0mM catechol in the presence of 1.67 mM imidazole at a glassy carbon electrode in aqueous solution containing 0.2 M phosphate buffer at a scan rate of 100mV s ⁻¹ -----	24

Figure 13. Variation of E_{pa} versus pH in electrochemical oxidation of 1.0 mM catechol in the presence of 1.67 mM imidazole at a glassy carbon electrode in aqueous solution containing 0.2 M phosphate buffer at a scan rate of 100 mV s^{-1} -----25

Figure 14. Typical voltammograms of 1.0 mM aqueous catechol in the presence of 1.67 mM imidazole at the glassy carbon electrode, in 0.2 M phosphate buffer of pH 7.0 at scan rates of 10,25, 50, 80,100, 200, 250,350, 500, 800,1000 mVs^{-1} -----26

Figure 15. Variation of peak current ratio (I_{pa}/I_{pc}) versus scan rate in electrochemical oxidation of 1.0mM catechol in the presence of 1.67 mM imidazole at the glassy carbon electrode in 0.2 M aqueous phosphate buffer of pH 7.0-----27

Figure 16. Variation of $I_{pa}/v^{1/2}$ versus scan rate in electrochemical oxidation of 1.0 mM catechol in the presence of 1.67 mM imidazole at the glassy carbon electrode in 0.2 M aqueous phosphate buffer of pH 7.0-----27

Figure 17. Variation of peak current ratio (I_{pc}/I_{pa}) versus scan rate in electrochemical oxidation of 1.0 mM catechol in the presence of 1.0 mM 2 at the glassy carbon electrode in 0.2 M aqueous phosphate buffer of pH 7.0-----28

Figure 18. Variation of E_{pc} versus scan rate in electrochemical oxidation of 1.0 mM catechol in the presence of 1.67 mM imidazole at the glassy carbon electrode in 0.2 M aqueous phosphate buffer of pH 7.0-----29

Figure 19. Variation of E_{pc} versus scan rate in electrochemical oxidation of 1.0 mM catechol in the Presence of 1.67 mM imidazole at the glassy carbon electrode in 0.2 M aqueous phosphate buffer of pH 7.0-----29

Figure 20. Variation of E_{pa} versus scan rate in electrochemical oxidation of 1.0mM catechol in the presence of 1.67mM imidazole at a glassy carbon electrode in aqueous solution containing 0.2 M phosphate buffer of pH 7.0-----30

Figure 21. Variation of ΔE_p versus scan rate in electrochemical oxidation of 1.0 mM catechol in the Presence of 1.67 mM imidazole at the glassy carbon electrode in 0.2 M aqueous phosphate buffer of pH 7.0-----30

Figure 22. Variation of experimental I_{rev}/I_{fwd} as a function of interpolated $\log k_f\tau$ -----33

Figure 23. Variation of experimental peak potential as a function of λ -----33

List of scheme page

Scheme 1 -----5

Scheme 2 -----7

Scheme 3 -----31

List of figure page

Table 1 -----32

Abstract

Electrochemical oxidation of catechol has been studied in the presence of imidazole as nucleophile in aqueous solution, using cyclic voltammetry. The results indicate the participation of catechol in 1, 4- Michael reaction with imidazole to form the corresponding catechol thioethers. Based on the observed EC mechanism, the homogeneous rate constants (k_{fcal}) of the reaction of *o*-benzoquinone with imidazole were estimated by fitting the theoretical working curve with the experimental working curve.

Key words: EC mechanism, cyclic voltammetry, catechol and imidazole.

1. Introduction

1.1. Coupled Chemical Reaction

A heterogeneous electron transfer reaction may be accompanied by a homogeneous chemical reaction. Particularly a reactive intermediate of a redox reaction is more susceptible to coupled reactions. An electrode reaction which is coupled to a homogeneous chemical reaction exhibits different behavior than a simple electron transfer reaction. Cyclic voltammetry (CV) may be used to diagnose such a 'complex' reaction. For a complex reaction a variety of possibilities exist including chemical reactions preceding or following a reversible or irreversible electron transfer. In one special case a chemical reaction is sandwiched between two electron transfer reactions (ECE mechanism). Some times a substance is intentionally added to a solution of the electroactive substance in order to study the rate of homogeneous reaction and the nature of interaction of the original substrate. The results of CV studies are helpful in interpreting the sequence of electron transfer and chemical reactions at the interface. Mechanistic studies require a knowledge of the nature of intermediate(s) produced, effect of additive on the substrate and the speed of the reaction(s) involved. The interest in mechanism elucidation has accelerated the development of various electrochemical techniques. Moreover coupling of spectroscopic techniques with electrochemical techniques has enabled precise monitoring of several coupled reactions.

Diagnosis of coupled chemical reactions is often based on the relative heights of the anodic and cathodic peak currents. Nicholson and Shain [1] have given tables of current functions from which the peak currents can be calculated for coupled chemical reactions. With the advancement in computer technology, digital simulation has proved a very useful tool to characterize the voltammograms or spectra for selected electrochemical reactions alone or coupled to homogeneous chemical reactions.

One of the most important applications of cyclic voltammetry is for the qualitative diagnosis of a chemical reaction that precedes or follows a redox process. Such reaction mechanisms are commonly classified by using the letters E and C (for redox and

chemical steps, respectively) in the order of the steps in the reaction scheme. The occurrence of such chemical reactions, which directly affect the available surface concentration of the electroactive species, is common to redox processes of many important organic and inorganic compounds. Changes in the shape of the cyclic voltammograms, resulting from the chemical competition for the electrochemical reactant or product, can be extremely useful for elucidating these reaction pathways and for providing reliable chemical information about reactive intermediates [2].

Electrochemical reactions, which are heterogeneous reactions at the interface electrode–electrolyte, are intrinsically more complex than typical (thermal) chemical transformations (Figure 1). We mostly neglect the exact structure of the interface in the following description. Transport of the substrate from the bulk of the electrolyte to the electrode plays an important, often rate-determining role. The electron transfer step occurs at the interface. The product of the redox reaction is transported back to the bulk. Purely chemical reactions may precede or follow these steps. Specific interactions of any species present in the electrolyte with the electrode surface leads to adsorption, which may considerably influence the overall process [3].

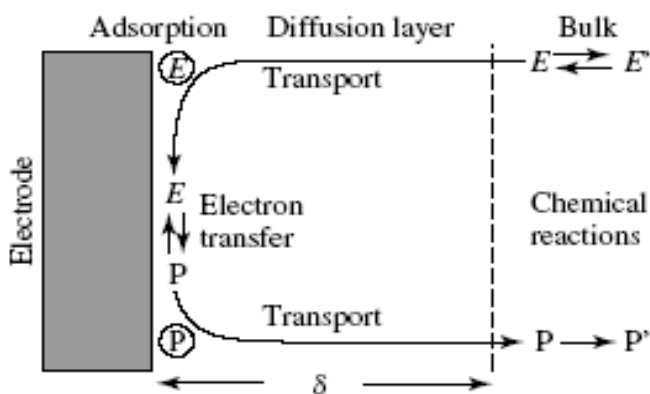


Figure 1. Steps constituting a typical organic electrode reaction; E, E': substrate, P, P': product; circles indicate adsorbed molecules.

1.2. Literature review

Electrochemistry provides very interesting and versatile means for the study of chemical reactions. Recently, the terms molecular electrochemistry or dynamic electrochemistry have been used for that part of electrochemistry that studies the mechanistic events at or near an electrode on a molecular level. The majority of organic electrode reactions are characterized by the generation of a reactive intermediate at the electrode by electron transfer and subsequent reactions typical for that species. These are often assumed to occur in a homogeneous solution, and not at the electrode surface itself.

The main goal of the electrochemical studies is the elucidation of the sequence of electron transfer and chemical reactions that occur near the electrode surface and their applications to electrosynthesis of organic compounds. The electrochemical generation and study of the intermediates may be advantageous because of the mild reaction conditions employed and the additional selectivity introduced in controlled-potential experiments [4]. Among the organic compounds, catechols (1) can be easily oxidized to the corresponding reactive *o*-benzoquinones mainly due to their low oxidation potentials. It is worth mentioning that catechols are used in a variety of applications including photography, dyeing, rubber and plastic production and pharmaceutical industry [5]. In addition, catechol derivatives play an important role in mammalian metabolism, and many compounds of this type are known to be secondary metabolites of higher plants. Also, many drugs such as doxorubicin, daunorubicin and mitomycin C which are used in cancer chemotherapy contain quinones. The catechol derivatives are a promising group of compounds which may lead to the discovery of selective acting, biodegradable agrochemicals having high human, animal and plant compatibility and, thus, worthwhile for further investigation. On the other hand, because electrochemical oxidation very often parallel the cytochrom catalyzed oxidation in liver microsomes, it was interesting to study the anodic oxidation of catechol derivatives in different conditions [6]. In recent years researchers have been mainly focused on the electrooxidation of catechols to produce *o*-benzoquinones as reactive intermediates in many useful homogeneous reactions. Thus, based on these valuable experiences, here we wish to focus on the

mechanistic study of homogeneous reactions coupled with electrochemical oxidation of catechols.

Electrochemical oxidation of catechols has been studied by many authors [7-10]. Electrochemical oxidation of catechols leads to the *o*-quinone as the first oxidation product. Electrochemical study on a glassy carbon electrode using cyclic voltammetry has shown that the first oxidation step involved a number of electrons per molecule equal to two which likely correspond to the formation of *o*-quinone [11]. The widespread availability and ease of oxidation of catechols in the presence of other functionalities make these compound attractive substrates for oxidative functionalization reactions. Electrooxidation of catechols and reactions of formed *o*-quinone with nucleophiles are well known and often comprise useful synthetic processes [12-16].

Electrochemical oxidation of catechols in the presence of phenyl-Meldrum's acid as a nucleophile in aqueous solution has been studied in detail by means of cyclic voltammetry and controlled potential coulometry. The results indicate that the *o*-benzoquinone derived from catechols participates in 1, 4-Michael addition reaction with phenyl-Meldrum's acid to form corresponding products [17].

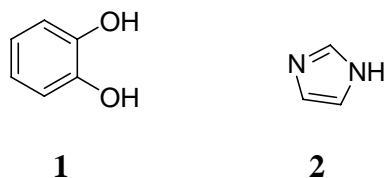
O-benzoquinones are extremely reactive compounds and have been utilized as important intermediates for the synthesis of various biologically active products. *O*-Benzoquinones are well known to react with nucleophiles following a 1, 4-Michael addition reaction or with diverse dienophiles performing a [4+2] cycloaddition [18].

Because most of *o*-benzoquinones are unstable (in contrast to *p*-benzoquinones), they are generally prepared in situ from their precursors, namely, catechols and 2-methoxyphenols. Organic electrochemical synthesis in aqueous medium provides an alternative strategy for the transformation of *o*-benzoquinones. Catechol can be oxidized electrochemically to the corresponding highly active *o*-benzoquinones, followed by a Michael addition reaction when nucleophiles are present in the system. Electrochemical processes use electrons as oxidants and thus avoid the utilization of toxic metal-based reagents. Also, such transformations are performed under mild reaction conditions, such as ambient temperature and normal pressure. From the viewpoint of green chemistry, it

would be more attractive [19, 20] to generate in situ *o*-benzoquinones through electrochemical methods. Indeed, this approach was investigated firstly by Tabakovic et al. [21] and then by Nematollahi and coworkers [22–26]. They investigated the anodic oxidation of catechols in the presence of different nucleophiles, such as C–H acids, amines, thiols and sulfinic acids, and obtained the corresponding coumestans, benzofurans and substituted catechols. Recently researchers demonstrated that the electrochemically formed *o*-benzoquinone also undergo [4+2] cycloaddition reaction with cyclopentadiene [27].

A vast number of quinones with great structural diversity are provided by nature, some of which play a major role in the redox electron-transport chains of living system [28-31]. In addition, many drugs such as doxorubicin, daunorubicin and mitomycin C in cancer chemotherapy contain quinones, whereas various other quinones have found uses in industry [32, 33].

As reported in the literature [34, 35, 36, 37, 38], the electrochemical oxidation of catechol in different conditions leads to the formation of final products *via* various mechanisms such as *CE*, *EC'*, *EC*, *ECE*, *ECEC*, *etc.* The mechanism depends on catechol type, nature of nucleophile, electrode potential and electrolysis medium. Catechol is known as a polyphenol in which two hydroxyl groups are substituted onto benzene ring. The other four remaining substituents are important parameters on determining the reaction mechanism. The presence of poor leaving groups or bulky groups on the reactive positions of electrochemically generated *o*-benzoquinone, *i.e.*, C-3 and C-4, inhibit or slowdown the coupled chemical reactions.



Scheme 1

Because of high reactivity of *o*-benzoquinone, the most coupled chemical reactions are following nucleophilic attacks and, thus, the nature of nucleophile plays an important role

in these reactions. The nucleophilic attacks that lead to the formation of catechol derivatives with more or less positive oxidation potentials are followed by more *E* steps and *C* steps depends on the structure of intermediates by *EC* reaction and even more *E* and *C* steps[39].

All of the chemical and electrochemical reactions of catechol derivatives depend on the nature of solvent and reaction media, specially the pH of the solution. The oxidation potential of catechol, reactivity of nucleophile, reactivity of catechol and produced quinone are strongly pH dependent. Solubility of final product or intermediate as well as the other reaction conditions is also important. For example low solubility or insolubility of intermediate inhibits the following chemical reactions [39].

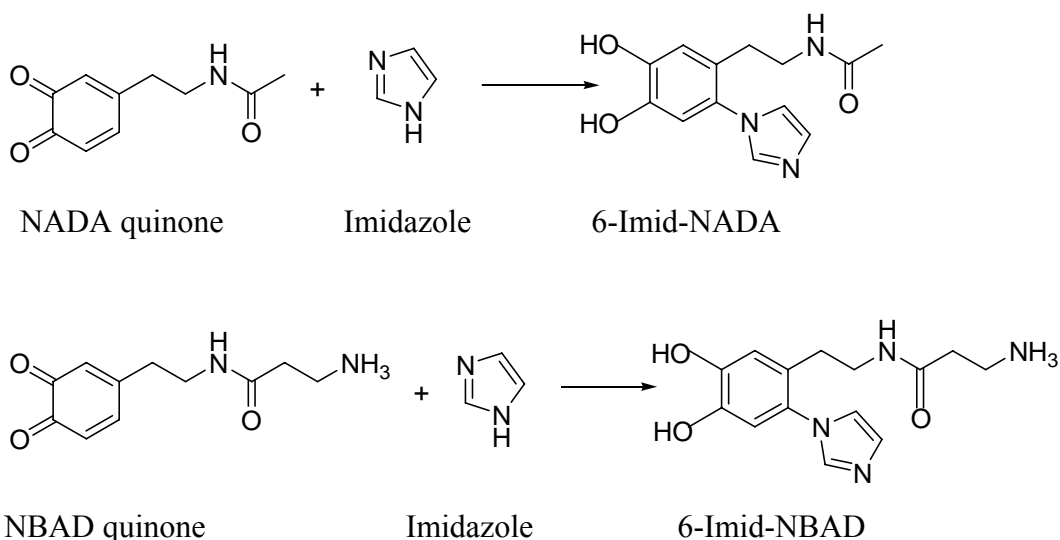
The existence of nitrogen nucleophile in imidazole (**2**) (scheme **1**) and biological media makes their investigations very important, particularly from their anti-oxidation and/or pro-oxidation properties when they attach to cellular species [40]. It is well-known that catechols can be oxidized electrochemically to *o*-benzoquinones. The *o*-benzoquinones formed are quite reactive and can be attacked by nucleophiles. In this connection, the electrochemical oxidation of catechols in the presence of a variety of nucleophiles such as thiotriazines [41-44], barbituric acids [45], 4-hydroxy-6-methyl-2-pyrone [46], 2-mercaptopyridine [47], 2-mercaptobenzoxazole [48], 3-mercapto-1,2,4-triazole [49], nitrogen and carbon nucleophiles[50], 4-amino-3-methyl-5-mercapto-1,2,4-triazole [51] 1-phenyl-5-mercaptotetrazole [52], 2-thiazoline-2-thiol [53] and 6- mercaptopurine [54] and 1-methylimidazole-2-thiol [55] have been studied using cyclic voltammetry and controlled-potential coulometry.

The electrochemical oxidation of catechols [47-56] has been studied and it has been shown that these compounds can be oxidized to related *o*-benzoquinones. The electrochemically generated *o*-benzoquinones are quite reactive and can be attacked by a variety of nucleophiles under various mechanisms such as *EC*, *CE*, *EC'*, *ECE*, *ECEC*, etc. The mechanistic pathways and final products depend on some parameters such as electron withdrawing or donating properties of nucleophile, electrolysis medium (solvent, acidity or pH) and nature of catechol. The results revealed that the quinones derived from

catechols participate in a Michael type addition reaction *via* an *EC* mechanism converted to the corresponding catechol derivatives.

In order to obtain some kinetic information for the system, the scheme for the electrochemical oxidation of catechols in the presence of nitrogen, carbon and thiols nucleophile were proposed and tested by digital simulation [55, 56]. The k_{obs} values for the reaction of *o*-benzoquinone with nucleophile were estimated by comparison of the simulation results with experimental cyclic voltammograms at various pH and scan rates. The simulation was performed based on an EC mechanism and the calculated value of observed homogeneous rate constant (k_{obs}) for reaction of *o*-benzoquinone with nucleophile was dependent on the nature and position of the substituted group on the catechol ring. The presence of an electron-donating group such as tertbutyl on catechol ring causes a decrease in k_{obs} [55].

A typical reaction of substituted *o*-quinones with imidazole is shown in scheme 2[57].



Where NADA stands for N-acetyldopamine and NBAD stands for N-β-ananyldopamine.

Scheme 2

1.3. Objective of the study

The objective of this project work is to carry out a cyclic voltammetric study of an electron transfer followed by a chemical reaction (EC mechanism) and to determine the kinetic parameters of the preceding homogeneous chemical reaction. The system investigated was the oxidation of catechol in the presence of imidazole as a nucleophile.

2. Characterization of chemical reactions coupled with electron transfer by cyclic voltammetry

2.1. Basics of cyclic voltammetry

Among many electrochemical techniques presented for the study of chemical reactions, cyclic voltammetry has become a very popular technique for initial electrochemical studies of new systems. It is easy to apply experimentally, readily available in commercial instruments and has proven as very useful tool in obtaining information about fairly complicated electrode reactions. Cyclic voltammograms are frequently and routinely used today to define the redox properties of newly synthesized organic compounds, similar to the use of NMR spectra for structural characterization [58]. The time scale of a cyclic voltammetry experiment is determined by the scan rate, *i.e.*, increasing scan rate decreases the experimental time scale; therefore, an important parameter in determining the effect of chemical reaction is the ratio of rate constant of chemical reaction to the scan rate, k/ν [2]. The detailed quantitative study of the chemical reactions coupled with electron transfer has been reported by Nicholson and Shain [1]. More complicated systems, involving slow heterogeneous kinetics, coupled homogeneous reactions or equilibria or more complex forms of mass transfer have been most easily treated by digital simulation. All of these results will often allow the defining of reaction steps.

The voltammetric current-potential curve is more mathematically challenging, but several solutions of the appropriate differential equations have appeared during the past three decades. Nicholson and Shain[1] revolutionized the voltammetric experiment with their elegant development and demonstration of linear-sweep and cyclic voltammetry.

In their approach the current-potential curve is presented as

$$i = nFAC^b(\pi Da)^{1/2}\chi(at) \quad (1)$$

where A is the area, C^b is the bulk concentration, D is the diffusion coefficient and $\pi^{1/2}\chi(at)$ is the current function for charge transfer followed by an irreversible chemical reaction.

The relation between $\pi^{1/2}\chi(at)$ and $n(E-E_{1/2})$ is given in tabulated form, a is defined by

$$a = nFv/RT = nv/0.026 [59].$$

and $E_{1/2}$ is the half-wave potential of the electrochemical process. For simplicity the term $\pi^{1/2}\chi(at)$ can be presented as χ_{rev} and equation(1) takes the form

$$i = nFAC^b (Da)^{1/2}\chi_{rev} \quad (2)$$

For a given potential (E) the value of χ_{rev} can be obtained from Nicholson and Shain's[1] table. A similar approach was used to obtain quantitative relations of irreversible processes as well as for those complicated chemical reactions.

For reversible process the peak potential can related to the polarographic half-wave potential $E_{1/2}$ by the expression

$$E_p = E_{1/2} - 1.11 \frac{RT}{nF} = E_{1/2} - 0.0285 \text{ at } 25^0\text{c} \quad (3)$$

Another useful parameter of the voltammetric curves is the half-peak potential $E_{p/2}$, which is the potential at which the registered current reaches half its maximum value. For a reversible process $E_{1/2}$ is located half way between E_p and $E_{p/2}$.

The ratio of peak current for the cathodic process relative to the peak current for the anodic process is equal to unity for reversible electrode process. For measurement of the peak current for the anodic process, the extrapolated baseline going from the foot of the cathodic wave to the extension of this cathodic current beyond the peak must be used as a reference, as shown in Figure 2.

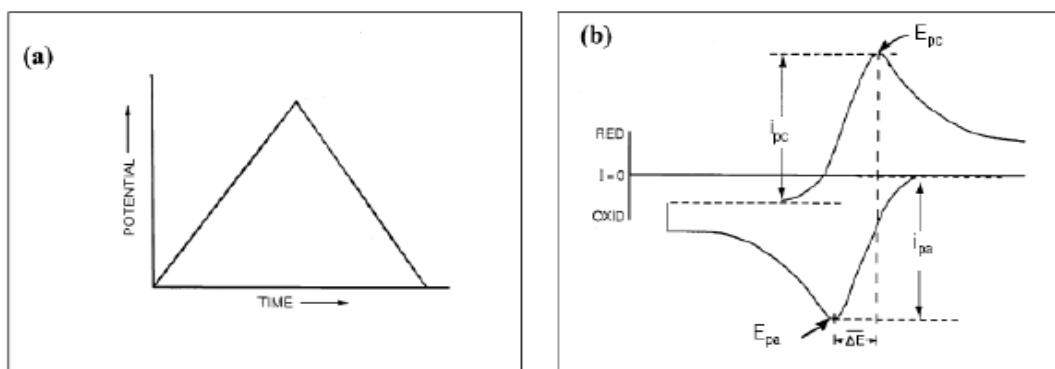


Figure .2 a) Excitation waveform and b) response obtained for the reversible by cyclic Voltammetry

The difference in the peak potentials between the anodic and cathodic waves of the reversible process is given by the relationship

$$|\Delta E_p| = |E_{pa} - E_{pc}| = \frac{0.059}{n} \quad \text{at } 25^\circ\text{C} \quad (4)$$

which provides a rapid and convenient means for determining the number of electrons involved in the electrochemical reaction. For a reversible system i_p is a linear function of $v^{1/2}$, and also E_p is independent of v .

The peak current for an irreversible reduction may be expressed in terms of a heterogeneous rate constant k_s and the peak potential by the relation

$$i_p = 0.227nFAC^b k_s \exp\left[\frac{-\alpha n_\alpha}{RT}(E_p - E^\circ)\right] \quad (5)$$

where k_s represents the heterogeneous rate constant of the electrode process for the condition that the electrode has a potential equal to the formal potential for the electrode process E° , n_α represents the number of electrons in the rate-controlling step and α is the transfer coefficient (normally a value between 0.3 and 0.7). A somewhat simpler form of this expression is possible if the instantaneous current of the wave is measured at a point that is less than 10% that of the peak current. For this condition the measured current is related to the kinetics parameters by the expression [59].

$$i = nFAC^b k_s \exp\frac{-\alpha n_\alpha F}{RT}(E_p - E_i) \quad (6)$$

where E is the potential at the measured current and E_i is the potential at which the scan was initiated.

Because of the dynamic nature of voltage-sweep voltammetry, irreversible processes give the following expression for the peak current

$$i_p = 2.99 \times 10^5 n(\alpha n_\alpha)^{1/2} AD^{1/2} C^b v^{1/2} \quad (7)$$

The value of αn_α can be evaluated by taking the difference between the peak potential and the half-peak potential:

$$E_p - E_{p/2} = -1.85 \frac{RT}{\alpha n_\alpha F} = \frac{-0.048}{\alpha n_\alpha} \quad \text{at } 25^\circ\text{C} \quad (8)$$

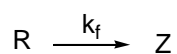
An alternative approach is to scan the voltammogram at two different rates. Under these conditions α and n_α may be evaluated by the expression

$$(E_p)_2 - (E_p)_1 = \frac{RT}{\alpha n_\alpha F} \ln \sqrt{\frac{v_1}{v_2}} \quad (9)$$

For irreversible systems the peak potential is shifted toward more negative potential by about 0.030V for a decade increase in the scan rate (equation 9). By analogy, a peak of an anodic process is shifted toward more positive potentials.

The most characteristic feature of a cyclic voltammogram of a totally irreversible system is the absence of a reverse peak. However, it does not necessarily imply an irreversible electron transfer but could be due to a fast following chemical reaction [59].

2.2. E_rC_i mechanism



This mechanism contains one electron transfer step followed by a coupled chemical reaction. The cyclic voltammogram observed depends on the relative rates of the two steps. The simplest situation is when the electron transfer is totally irreversible; the presence of chemical reaction has no effect on the voltammogram obtained and no kinetic data related to the chemical reaction can be derived. The effect of a following chemical reaction is of course greatest on the reverse sweep where R is reoxidized. If the chemical reaction is fast, R is rapidly removed from the region near the electrode.

Figure 3 shows normalized theoretical cyclic voltammograms for the case of reversible electron transfer followed by irreversible chemical reaction for a range of values of the variable λ given by, $\lambda = k(RT/nF)/\nu$ [60].

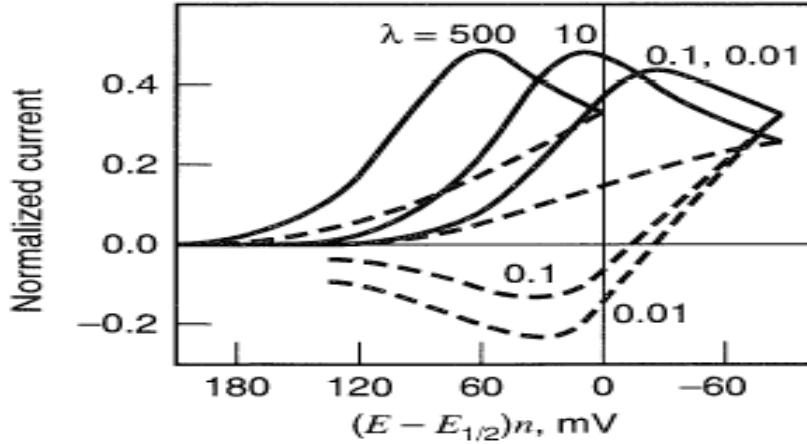


Figure 3. Cyclic voltammograms for E_rC_i case at 25°C. The current scale is normalized to the peak current, for several values of $\lambda = k(RT/nF)/\nu$ [61].

In the region where no reverse peak is observed, the pure kinetic zone, it can be shown that the chemical reaction has the effect of shifting the E_{pc} value for the reversible electron transfer. This is because the coupled chemical reaction reduces the concentration of R at the surface from the value it would have had for a simple electron transfer reaction. The electrode reaction therefore has to work harder to maintain Nerstian equilibrium at the surface. However, the peak shifts back $30/n$ mV in a negative direction for each ten fold increase in scan rate, provided the chemical reaction is first order in the intermediate produced at the electrode surface. Eventually as the sweep rate is increased a reverse peak starts to appear, and the rate of change of E_p with sweep rate decreases. The ratio of the cathodic to anodic peak current continues to increase with the sweep rate until eventually reversible behavior is observed. It is from the region where a reverse peak is observed, but the ratio of $|I_{pa}/I_{pc}|$ is less than one, that kinetic data can be obtained. This is the region where $5 \geq \lambda \geq 0.1$ (a relatively small range) and in the kinetic region, E_p given by

$$E_p = E_{1/2} - \frac{RT}{nF} 0.780 + \frac{RT}{2nF} \ln \lambda \quad (10)$$

The rate constant is obtained by comparing experimental $|I_{pa}/I_{pc}|$ ratios with the working curve described by Nicholson and Shain [1] where this ratio is plotted as a function of $\log k_f \tau$ where τ is the time required to traverse the potential range from the polarographic half wave potential ($E_{1/2}$) to the switching potential E_λ , (the potential at which the sweep is reversed). Such a working curve is shown in figure 4.

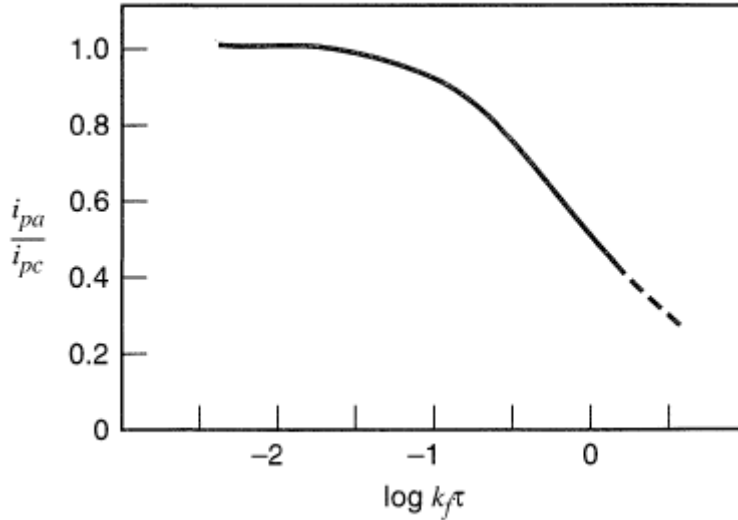


Figure 4. Ratio of anodic to cathodic peak current as a function of $k_f \tau$, where τ is the time between $E_{1/2}$ and the switching potential E_λ [61].

To insure reliable values of the rate constant a range of switching potentials and sweep rates should be used. The value of the half wave potential can be obtained from data under reversible conditions. E_{pc} and $E_{pc/2}$ are related by equation (11).

$$E_{pc} - E_{pc/2} = -1.109 \frac{RT}{nF} = \frac{-28.5}{n} mV \quad \text{at } 25^0c \quad (11)$$

An alternative approach based on peak potential measurements arises from the kinetics analysis. For values of $\log \lambda < -0.95$ the behavior corresponds to a diffusion controlled system, i.e. the peak potential does not shift with sweep rate, whilst for $\log \lambda \geq 0.28$, E_{pc} shifts 30 mV in a negative direction for each ten fold increase in scan rate. If experimental peak potential data obtained over a sufficiently wide sweep range are plotted as a function of $\log v$, there should be horizontal linear region (diffusion control)

an oblique linear region (kinetic control) and a curved region (mixed control) linking them. From the $\log v$ values at which the range occurs, the value of k can be found by using the λ values given above.

The peak, which is generally positive of the reversible E_p value because of the following reaction, shifts in a negative direction (toward the reversible curve) with increasing v (Figure 5).

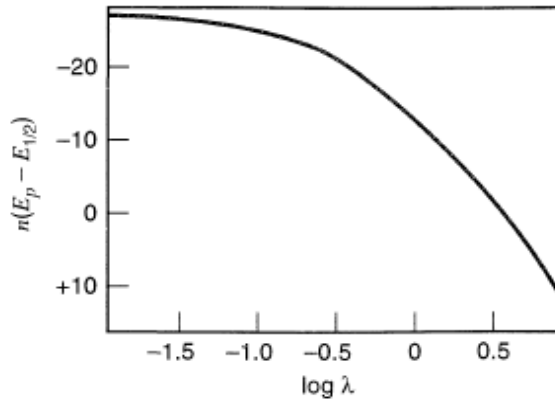


Figure 5. Variation of peak potential as a function of λ for the E_rC_i case [61].

2.3. Diagnostic test [60]

Diagnostic tests for a reversible electron transfer process at 25°C

1. $\Delta E_p = E_{pa} - E_{pc} = 59/n$ mV
2. $\Delta E_p = |E_p - E_{p/2}| = 59/n$ mV
3. $|I_{pa}/I_{pc}| = 1$
4. $I_p \propto v^{1/2}$
5. E_p is independent v
6. At potentials beyond E_p , $I^{-2} \propto t$

Diagnostic tests for a quasi-reversible electron transfer process at 25°C

1. $|I_p|$ increases with $v^{1/2}$ but is not proportional to it
2. ΔE_p is greater than $59/n$ mV and increasing v .
3. E_{pc} shifts negatively with increasing v .

Diagnostic tests for a totally irreversible electron transfer process at 25⁰C

1. no reverse peak
2. $I_{pc} \propto v^{1/2}$
3. E_{pc} shifts $-30/\alpha_c n \alpha$ mV for each decade increase in v
4. $|E_p - E_{p/2}| = 48/\alpha_c n \alpha$ mV

Diagnostic tests for EC mechanism at 25⁰C

1. $I_{pc}/v^{1/2}$ decreases slightly with increasing v
2. E_{pc} is positive of the value for the reversible case
3. E_{pc} shifts negatively with increasing v , in the pure kinetic region shifts by 30/mV per 10 fold increase in v

3. Experimental part

3.1. Reagents and chemicals

The reagents and chemicals used were Catechol (BDH Poole, England), imidazole (Sigma-Aldrich Co.Ltd, UK), disodium hydrogen phosphate (Wagtech International Ltd, UK), sodium dihydrogen phosphate (Riedel-deHaen, Germany), HCl (Riedel-deHaen, Germany), NaOH (BDH Poole, England).

3.2. Instrumentation

The cyclic voltammetry experiments were performed using the BAS 100A, electrochemical analyzer [Bioanalytical systems (BAS), USA], which was connected to a Dell computer (Pentium 4). A magnetic stirrer with a hot plate from Cole Palmer instrument company was also used for stirring in pH adjustments. The pH of the buffer solution was measured with a Hanna digital pH 301 meter with combination glass electrode. All the potentials are determined with respect to a Ag/AgCl (3.0MKCl) electrode as a reference electrode.

3.3. Electrolytic cells and electrodes

This work was performed using a three-electrode system with a one-compartment glass voltammetric cell, a Ag/AgCl (3.0MKCl) electrode as a reference electrode and platinum wire as an auxiliary electrode. The working electrode was the glassy carbon electrode (GCE) with a diameter of 3mm.

3.4. Procedure

Supporting electrolyte of phosphate buffers (NaH_2PO_4 – Na_2HPO_4) in the pH range 4-8 were prepared from 0.2 M NaH_2PO_4 and 0.2 M Na_2HPO_4 in double distilled water. The pH of the solutions was adjusted by adding drops of concentrated HCl and NaOH. The working electrode was pretreated by polishing it with an alumina and rinsing in distilled water. Doubly distilled water was used through out the work. Finally, by adjusting all the

necessary parameters cyclic voltammetry measurements were run. All measurements were performed at room temperature.

4. Result and discussion

4.1. Electrochemical investigations of catechol

Electrochemical properties of catechol were studied by cyclic voltammetry. Cyclic voltammograms of 1.0 mM catechol in aqueous solution containing phosphate buffer (pH 7.00) at various potential scan rates are shown in Figure 6. As can be seen, there are two anodic peak (a_0) and (a), but the first anodic peak (a_0) may be the intermediate quinone. The second anodic peak (a) related to the oxidation of catechol to *o*-benzoquinone and one corresponding cathodic peak(c) related to reduction of *o*-benzoquinone to catechol.

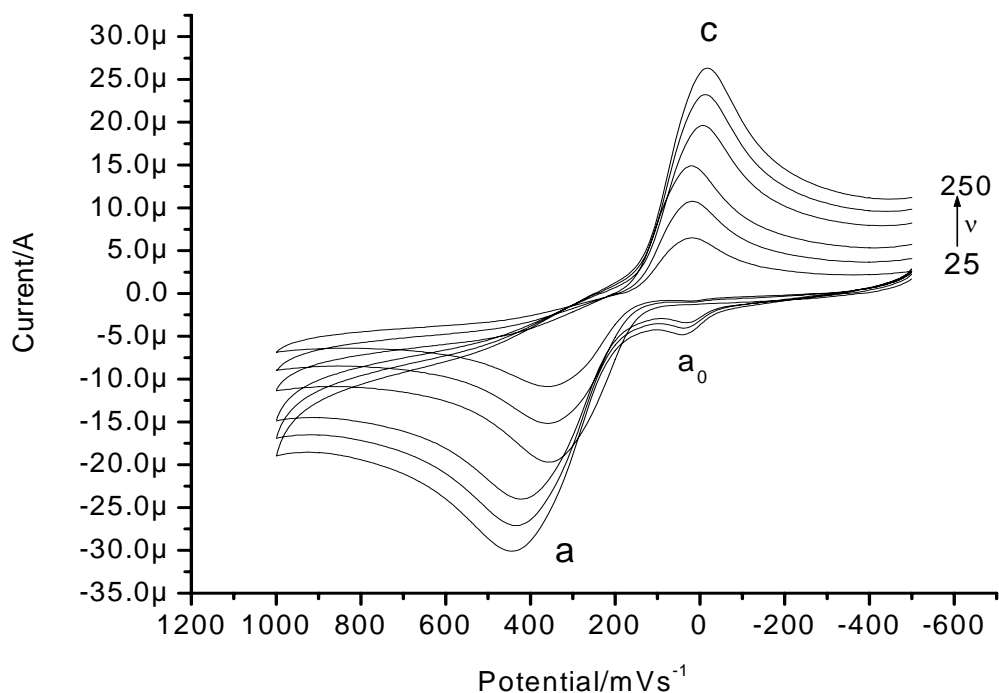


Figure 6. Typical voltammograms of 1.0 mM catechol at the glassy carbon electrode, in 0.2 M phosphate buffer of pH 7.0 at scan rates 25, 50, 100,150, 200, 250mV s⁻¹.

It is quite common for a process that is reversible at low sweep rates to become irreversible at higher ones after having passed through region known as quasi-reversible at intermediate values. This transition from reversibility occurs when the relative rate of the electron transfer with respect to that of mass transport is insufficient to maintain Nernstian equilibrium at the electrode surface. In quasi-reversible region both forward and backward reactions make a contribution to the observed current. This change from reversible, to quasi-reversible and finally irreversible behavior can readily be seen from a plot of I_p as a function of $v^{1/2}$ (square root of scan rate) as shown in Figure 7[60].

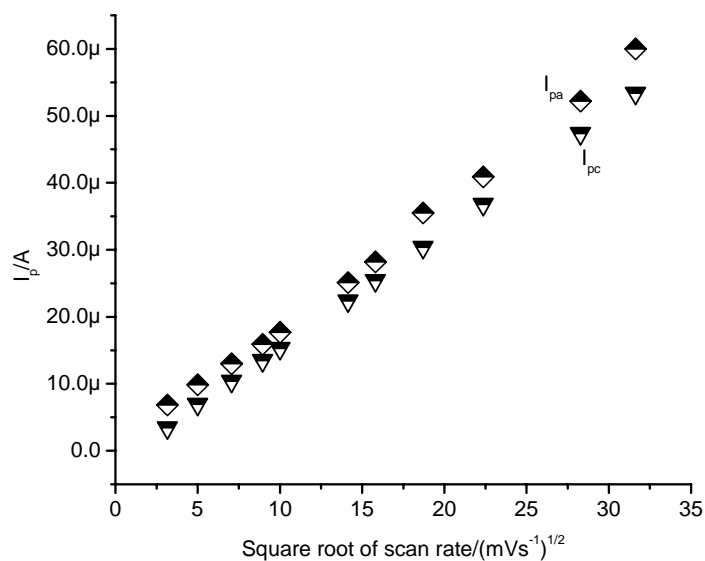


Figure 7. Variation of I_p versus square root of scan rate in electrochemical oxidation of 1.0mM catechol at a glassy carbon electrode in aqueous solution containing 0.2 M phosphate buffer of pH 7.0.

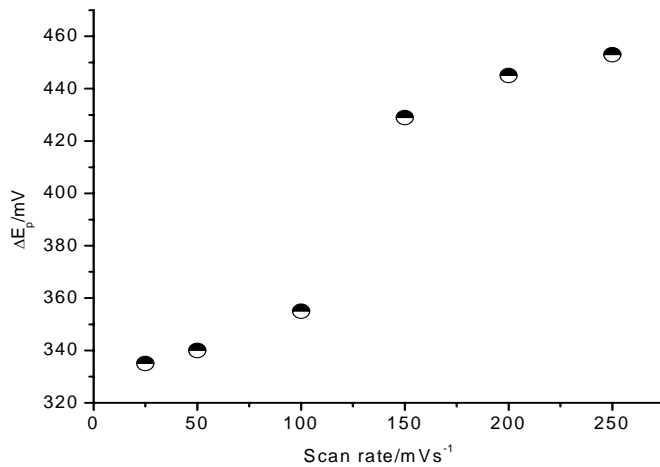


Figure 8. Variation of ΔE_p versus scan rate in electrochemical oxidation of 1.0mM catechol at a glassy carbon electrode in aqueous solution containing 0.2 M phosphate buffer of pH 7.0.

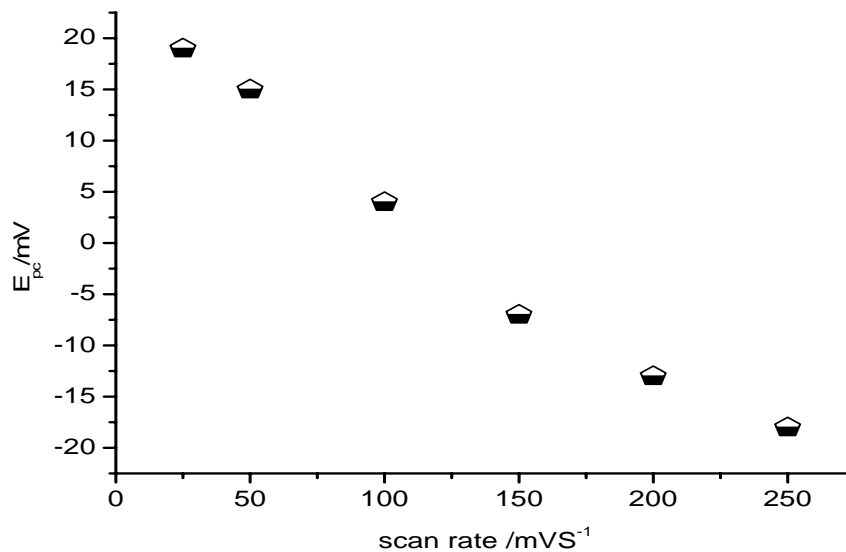


Figure 9. Variation of E_{pc} versus scan rate in electrochemical oxidation of 1.0 mM catechol at a glassy carbon electrode in aqueous solution containing 0.2 M phosphate buffer of pH 7.0.

The peak separation potential, ΔE_p at different scan rate is greater than $59/n$ mv (Figure 8) and E_{pc} shifts negatively with increasing scan rate (Figure 9). These diagnostic citations fulfill the requirement for a quasi-reversible electron transfer process [60].

4.2. Electrochemical investigation of Catechol in the Presence of imidazole

The oxidation of catechol yields *o*-benzoquinone, which frequently undergoes nucleophilic attack. The nucleophile usually reacts by a 1, 4-Michael addition reaction to form a substituted *o*-benzoquinone. If the substituent is such that the potential for the oxidation of product is higher, the reaction will be complete after the first oxidation-addition process [62]. Cyclic voltammogram of 1.0 mM of catechol in aqueous solution containing 0.2 M phosphate buffer of pH 7.0 shows one anodic (a) and corresponding cathodic peak (c), corresponding to the transformation of catechol to *o*-benzoquinone and vice versa within a quasi-reversible two electron process (Figure 10, curve 3). A peak current ratio (I_{pc}/I_{pa}) of nearly unity, particularly during the recycling of potential, can be considered as criteria for the stability of *o*-benzoquinone produced at the surface of electrode under the experimental conditions. As it is shown in Figure 10, curve 2, in the presence of imidazole as a nucleophile causes there is an anodic potential shift with decrease in the anodic current of peak a_1 , and a decrease of the cathodic counterpart c_1 of the anodic peak a_1 . The positive shift of the anodic peak a_1 in the presence of imidazole, which is enhanced during the repetitive recycling of potential, is probably due to the formation of a thin film of product at the surface of the electrode inhibiting to a certain extent the performance of the electrode process [63]. In this Figure 10, curve 1, is the voltammogram of 1.67 mM of imidazole. For the reaction between *o*-benzoquinone and imidazole, please refer to scheme 3, page 31.

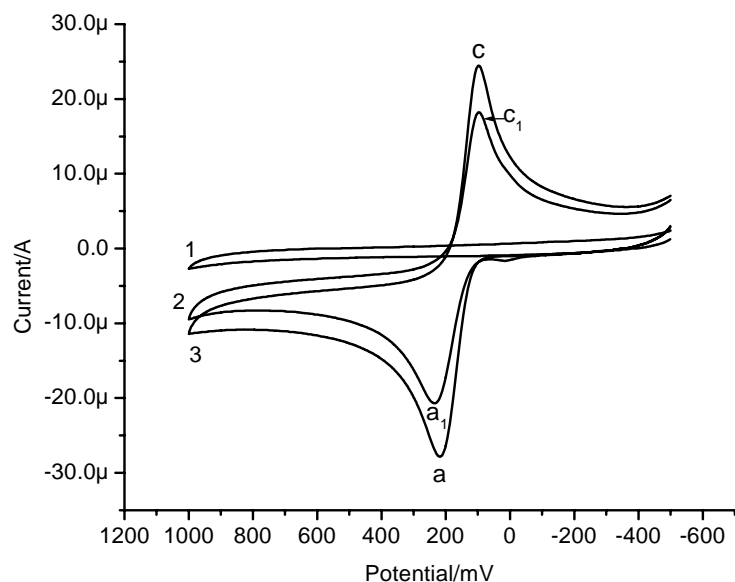


Figure 10. Cyclic voltammograms of 1.0 mM catechol in the absence (3) and presence of 1.67 mM imidazole (2), and that of a 1.67 mM imidazole in the absence of catechol (1) at the glassy carbon electrode in 0.2 M aqueous phosphate buffer of pH 7.0 at a scan rate of 100 mV s^{-1} .

4.3. Effect of pH

The oxidation of catechol in the presence of imidazole was studied by cyclic voltammetry at various pHs (Figure 11). The results show that the peak current ratio (I_{pc}/I_{pa}) increases with increasing pH up to 7.0 (Figure 12). This is related to protonation of imidazole at lower pHs and its subsequent inactivation towards a 1, 4-Michael addition. On the other hand, the basic media increases the rate of the coupling reaction between anion formed from deprotonation(s) of catechol and o-benzoquinone (dimerization reaction) [64]. Thus, because of the decreased rate of dimerization reaction and increased rate of the coupling reaction between deprotonated imidazole and o-benzoquinone, a solution containing 0.2 M phosphate buffer of pH 7.0 was selected as solvent system for the electrochemical study and synthesis of these aminoquinone derivatives (Figure 11).

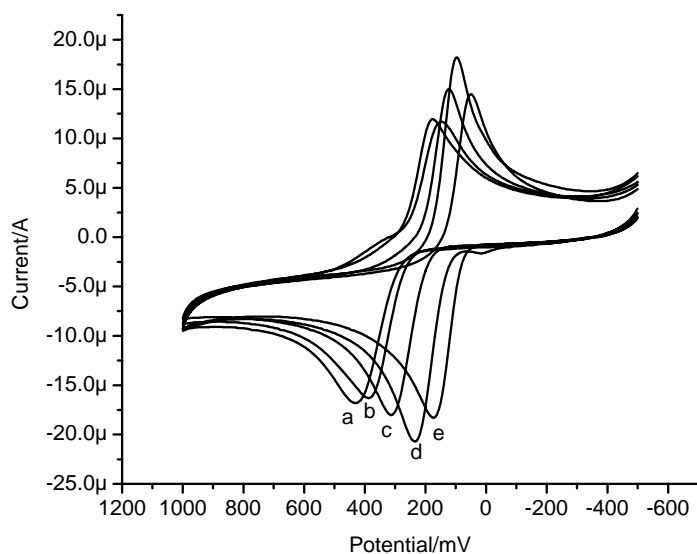


Figure 11. Cyclic voltammograms of 1.0 mM catechol in the presence of 1.67 mM imidazole at glassy carbon electrode at a scan rate of 100mVs^{-1} and various pH: (a) 4, (b) 5, (c) 6, (d) 7, (e) 8.

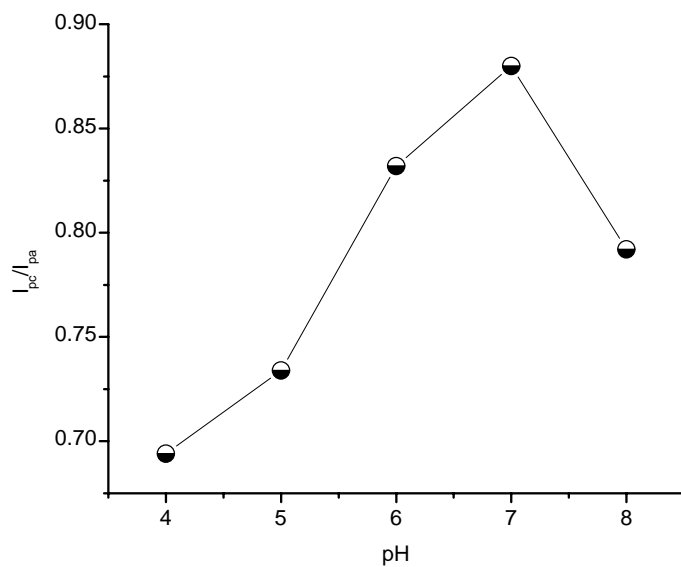


Figure 12. Variation of peak current ratio (I_{pc}/I_{pa}) versus pH in electrochemical oxidation of 1.0mM catechol in the presence of 1.67 mM imidazole at a glassy carbon electrode in aqueous solution containing 0.2 M phosphate buffer at a scan rate of 100 mV s^{-1} .

The dependence of E_{pa} on the solution pH shows a straight line (Figure 13) whose slope is -66.6mV pH^{-1} ($r = -0.9902$). This slope has been usually determined for phenolics systems in aqueous media, which stands for electrochemical reactions followed by deprotonation involving the same number of protons ($m \approx 2$) and electrons ($n \approx 2$) which was determined by equating the theoretical slope ($2.303mRT/2F$) with the experimental slope (-66.6mVpH^{-1}) [65, 66].

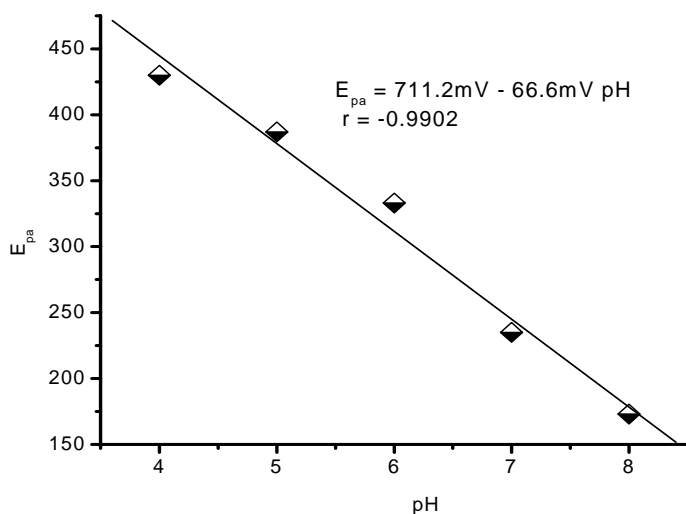


Figure 13. Variation of E_{pa} versus pH in electrochemical oxidation of 1.0 mM catechol in the presence of 1.67 mM imidazole at a glassy carbon electrode in aqueous solution containing 0.2 M phosphate buffer at a scan rate of 100 mV s^{-1} .

4.4. Effect of scan rate

The cyclic voltammograms of catechol in the presence of imidazole at various scan rates are shown in Figure 14. It is seen that proportional to the augmentation of potential sweep rate, the height of the cathodic (c) peak of catechol increases. A similar situation is also observed when the 3 to 1 concentration ratio is decreased. On the other hand, the decreasing current function and decreasing current ratio (I_{pa}/I_{pc}) with increasing scan rate are good indications of the reactivity of deprotonated imidazole toward o-benzoquinone (Figure 15).

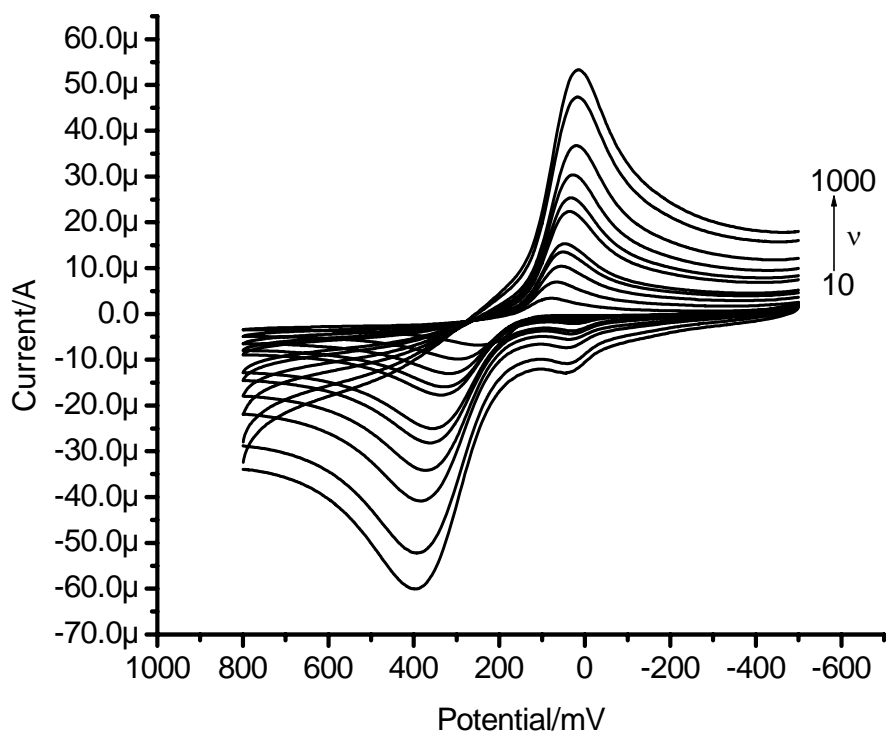


Figure 14. Typical voltammograms of 1.0 mM aqueous catechol in the presence of 1.67 mM imidazole at the glassy carbon electrode, in 0.2 M phosphate buffer of pH 7.0 at scan rates of 10, 25, 50, 80, 100, 200, 250, 350, 500, 800, 1000 mVs^{-1} .

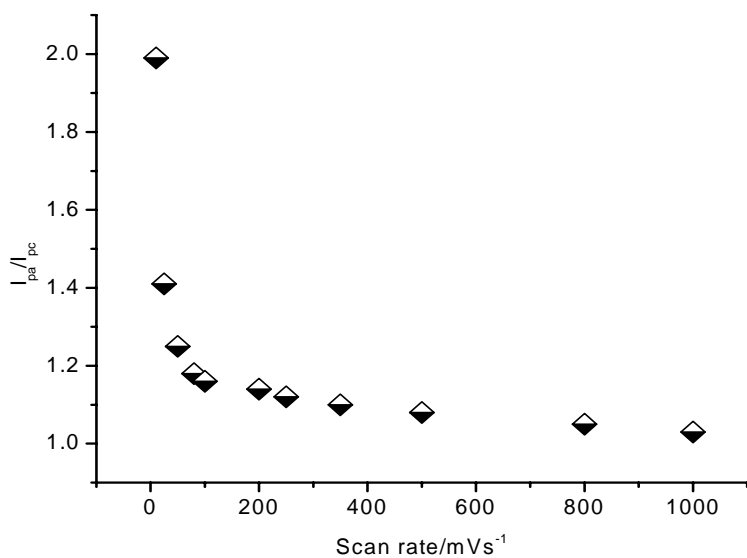


Figure 15. Variation of peak current ratio (I_{pa}/I_{pc}) versus scan rate in electrochemical oxidation of 1.0mM catechol in the presence of 1.67 mM imidazole at the glassy carbon electrode in 0.2 M aqueous phosphate buffer of pH 7.0.

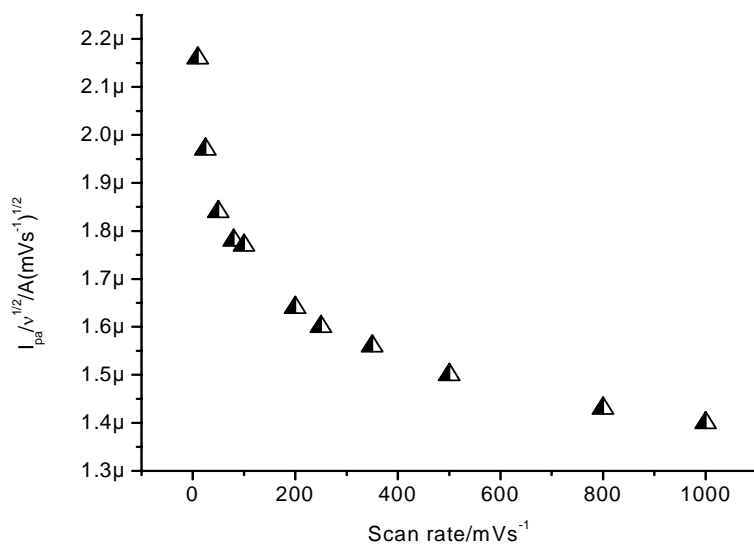


Figure 16. Variation of $I_{pa}/v^{1/2}$ versus scan rate in electrochemical oxidation of 1.0 mM catechol in the presence of 1.67 mM imidazole at the glassy carbon electrode in 0.2 M aqueous phosphate buffer of pH 7.0.

A decrease of the peak current function ($I_{pa}/v^{1/2}$) (Figure 16) as a function of scan rate is in good agreement with that of occurrence of a chemical reaction after the electron transfer process (EC mechanism).

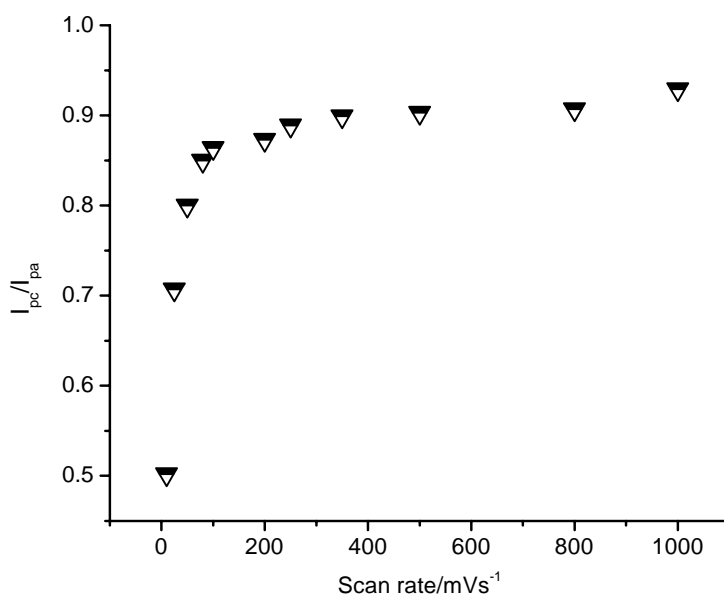


Figure 17. Variation of peak current ratio (I_{pc}/I_{pa}) versus scan rate in electrochemical oxidation of 1.0 mM catechol in the presence of 1.67 mM imidazole at the glassy carbon electrode in 0.2 M aqueous phosphate buffer of pH 7.0.

The increasing peak current ratio (I_{pc}/I_{pa}) with increasing scan rate (Figure 17) and decreasing of current function ($I_{pa}/v^{1/2}$) (Figure 16) with increasing scan rate have been adapted as being indicative of the EC mechanisms [46,66].

For irreversible homogeneous chemical reaction the cathodic peak potential (E_{pc}) is shifted toward more negative potential as the scan rate increases (Figure 18) and the relation between I_{pc} and square root of scan rate ($v^{1/2}$) is linear ($r = 0.99994$) (Figure 19). By analogy, a peak of an anodic process is shifted toward more positive potentials. These diagnostic citations fulfill the requirement for irreversible homogeneous chemical reaction [59].

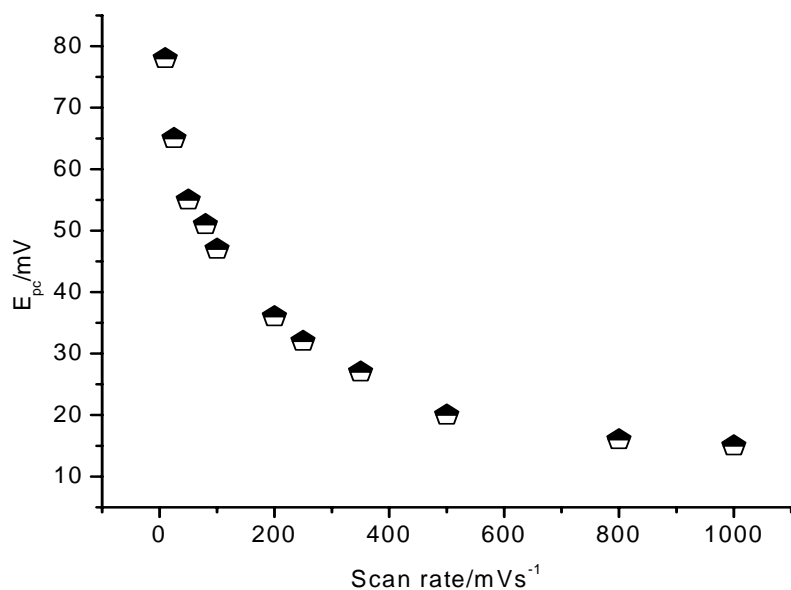


Figure 18. Variation of E_{pc} versus scan rate in electrochemical oxidation of 1.0 mM catechol in the presence of 1.67 mM imidazole at the glassy carbon electrode in 0.2 M aqueous phosphate buffer of pH 7.0.

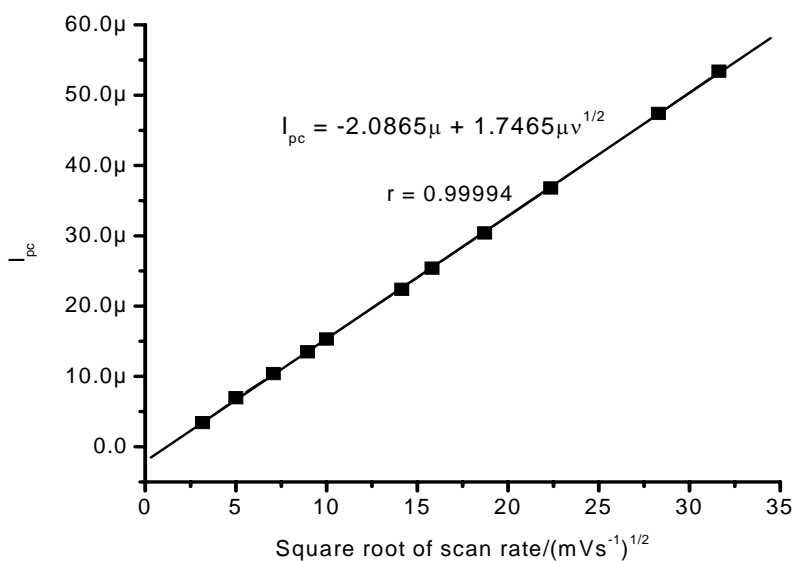


Figure 19. Variation of I_{pc} versus square root of scan rate in electrochemical oxidation of 1.0 mM catechol in the Presence of 1.67 mM imidazole at the glassy carbon electrode in 0.2 M aqueous phosphate buffer of pH 7.0.

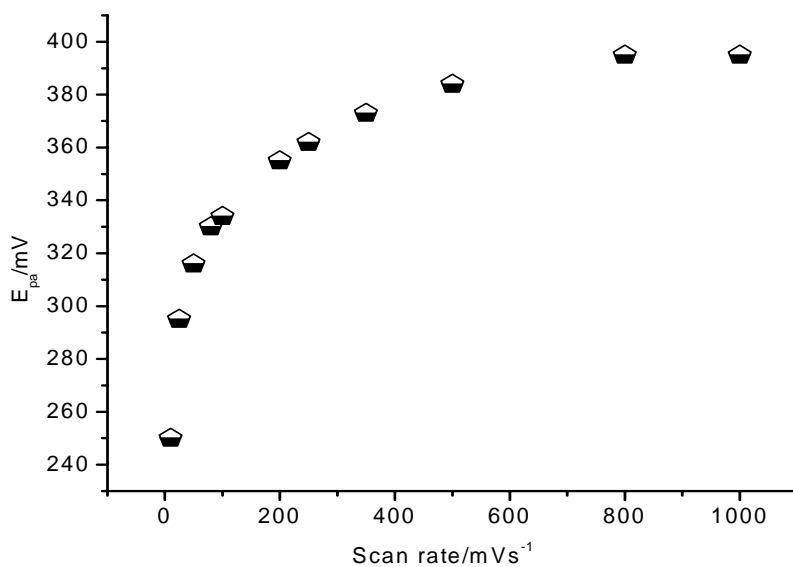


Figure 20. Variation of E_{pa} versus scan rate in electrochemical oxidation of 1.0 mM catechol in the presence of 1.67 mM imidazole at a glassy carbon electrode in aqueous solution containing 0.2 M phosphate buffer of pH 7.0.

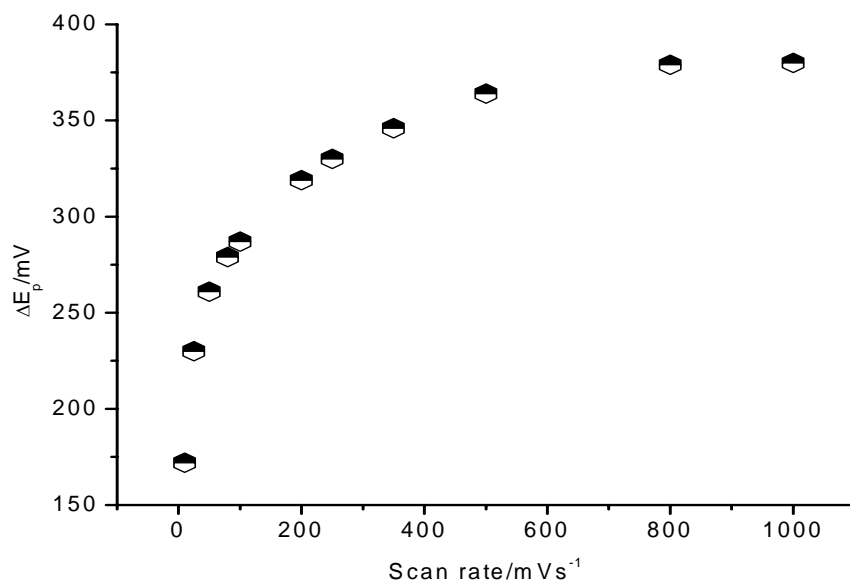


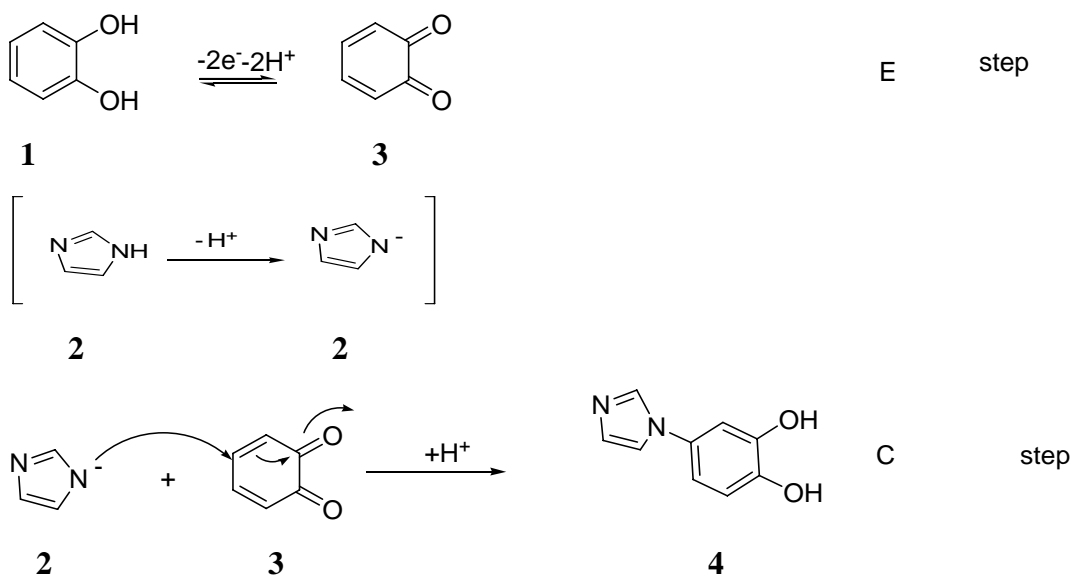
Figure 21. Variation of ΔE_p versus scan rate in electrochemical oxidation of 1.0 mM catechol in the Presence of 1.67 mM imidazole at the glassy carbon electrode in 0.2 M aqueous phosphate buffer of pH 7.0.

Increasing the scan rate shifts the anodic peak potential (E_{pa}) to more positive direction (Figure 20). This supports the irreversibility of the homogeneous chemical reaction. It was also observed that the potential difference ΔE_p was greater than $59/n$ and it increases with increasing scan rate (Figure 21); these indicate that the concentration of redox species cannot establish at the surface of the electrode according to the Nernst equation [67].

According to the obtained results, it seems that deprotonated form of imidazole participates in a 1, 4-Michael addition reaction with o-benzoquinone to result in the final product **4** (see scheme 3 below).

Mechanism

In the work of Adams and Co-workers [68] and Nematollahi and Co-workers [22, 23, 24, 26, 69], they have demonstrated that the anodic oxidation of catechol and its derivatives in aqueous medium affords o-benzoquinones by two electron ($2e^-$) anodic process, which undergo a Michael addition to form substituted catechol derivatives (by an EC type mechanism) in the presence of imidazole. Scheme 3 describes the anodic oxidation of catechol to the corresponding highly reactive o-benzoquinone which undergoes a Michael reaction with imidazole, to finally generate **4**.



Scheme 3

4.6. Kinetics study

The ratio of the currents, I_{rev}/I_{fwd} , can be conveniently measured by the empirical method of Nicholson and Shain [70], that requires the evaluation of I_{pa} , I_{pc} , and I_{λ} , where I_{λ} is the value of the current at the switching potential, E_{λ} (where the direction of the CV scan is reversed). These quantities are then used to obtain the current ratio, I_{rev}/I_{fwd} in equation. (12).

$$\frac{I_{rev}}{I_{fwd}} = \frac{I_{pc}}{I_{pa}} + 0.48 \frac{I_{\lambda}}{I_{pa}} + 0.086 \quad (12)$$

The electrochemical oxidation of catechol in the presence of imidazole is proposed and tested by the experimental cyclic voltammograms results with the theoretical working curve. On the basis of an EC mechanism, the calculated homogeneous rate constants (k_{fcal}) of reaction of *o*-benzoquinone with imidazole have been estimated by inserting the experimental I_{rev}/I_{fwd} into the theoretical working curve (Figure 4) to determine $k_f\tau$. From the experimental τ , the average value of k_f was then determined as $0.0646s^{-1}$. Figure 22 shows variation of experimental I_{rev}/I_{fwd} as a function of interpolated $\log k_f\tau$.

Table 1. I_{rev}/I_{fwd} values as a function of the theoretical and experimental values of $k_f\tau$.

$k_f\tau$ * (theort'l)	$\log k_f\tau$ * (theor)	I_{rev}/I_{fwd} * (theort'l)	I_{rev}/I_{fwd} (expt'l)	τ (expt'l)	Log $k_f\tau$ (interpolated)	$k_f\tau$ (interpolated)	K_f (calculated)/ s^{-1}
0.004	-2.3979	1.00	0.907	0.595	-1.013	0.097	0.813
0.023	-1.6383	0.986	0.901	0.743	-1.013	0.097	0.131
0.035	-1.4559	0.967	0.899	1.196	-0.959	0.109	0.091
0.066	-1.18046	0.937	0.893	1.714	-0.928	0.151	0.088
0.105	-0.97881	0.900	0.89	2.412	-0.959	0.109	0.040
0.195	-0.70997	0.828	0.863	3.023	-0.832	0.118	0.039
0.35	-0.45593	0.727	0.856	6.095	-0.821	0.147	0.024
0.525	-0.27984	0.641	0.85	7.619	-0.821	0.151	0.019
0.550	-0.25964	0.628	0.80	12.290	-0.704	0.198	0.016
0.778	-0.10902	0.551	0.707	24.80	-0.437	0.366	0.015

* Theoretical values [1, 70].

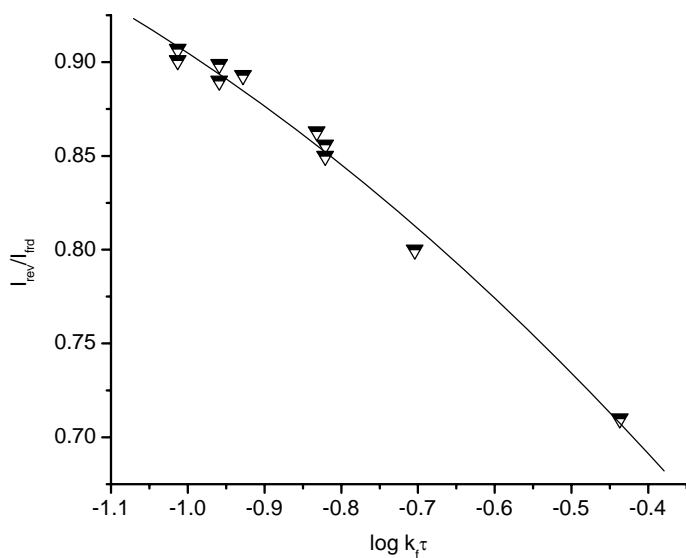


Figure 22. Variation of experimental I_{rev}/I_{frd} as a function of interpolated $\log k_f \tau$.

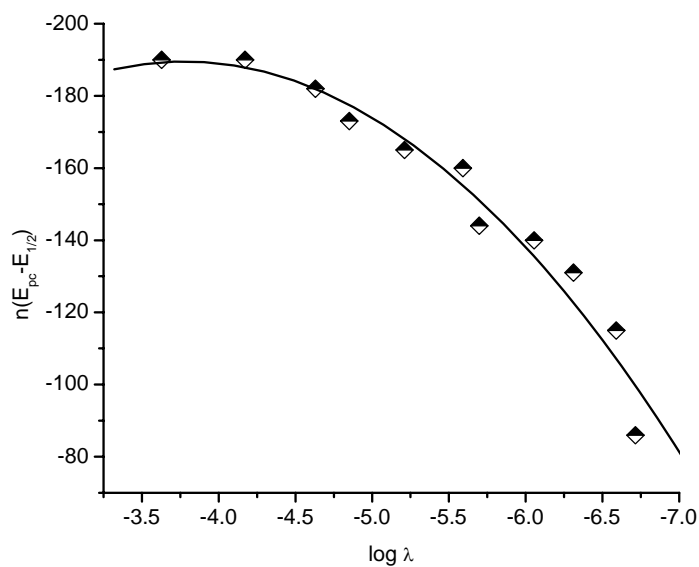


Figure 23. Variation of experimental peak potential as a function of $\lambda = k(RT/nF)/v$.

Using the value of k_{fcal} from the experimental result (table 1) the peak, which is generally positive of the reversible E_{pc} values because of the following reaction, shifts in a negative direction (to ward the reversible curve) with increasing scan rate (Figure 23), indicating an irreversible homogeneous chemical reaction[61].

5. Conclusion

The overall reaction mechanism for electrochemical oxidation of catechol in presence of imidazole is presented in Scheme 3. According to obtained results, the mechanism of electrooxidation reaction of catechol in the presence of imidazole is an EC mechanism. The kinetics of the reactions of electrochemically generated *o*-benzoquinone with imidazole was studied by cyclic voltammetric technique. The electrochemical oxidation of catechol in the presence of imidazole is proposed and tested by the experimental cyclic voltammograms results with the theoretical working curve. On the basis of an EC mechanism, the calculated homogeneous rate constants (k_{cal}) of the reaction of *o*-benzoquinone with imidazole estimated was 0.0646s^{-1} by fitting theoretical working curve with experimental working curve.

6. References

1. R.S.Nicholson and I. Shain, *Anal.Chem.*, 36(1964)706.
2. J. Wang, *Analytical Electrochemistry*, 2nd ed., Willey-VCH, New York, (2000).
3. E. Vieil, G. Cauquis, *J. Electroanal. Chem.*, 148(1983)183–200.
4. H. Lund, O. Hammerich, *Organic Electrochemistry*, 4th ed., Marcel Dekker, New York, (2001).
5. N. Schweigert, A.J.B. Zehnder, R.I.L. Eggen, *Environ. Microbiol.*, 3(2001) 81.
6. J.L. Bolton, E. Pisha, L. Shen, E.S. Krol, S.L. Iverson, Z. Huang, R.B. van Breemen, J.M. Pezzuto, *Chem. Biol. Interact.*, 106(1997)133.
7. S. Maldonado, S. Morin, K. J. Stevenson, *Analyst*, 131(2006)262.
8. M. D.Hawley; S. V.Tatawawadi, S. Piekarski, R. N. Adarns, *J. Am. Chem. Soc.*, 89 (1967) 447.
9. T.N. agaoka, T. Yoshino, *Anal. Chem.*, 58(1986)1037.
10. C. Ueda, D. Chi-Sing Tse, T. Kuwana, *Anal. Chem.*, 54(1982)850.
11. D.Nematollahi, D. Habibi, M. Rahmati, M. Rafiee, *J. Org. Chem.*, 69(2004)2637.
12. D. Nematollahi, E.Tammari, *J. Org. Chem.*, 70(2005)7769.
13. D. Nematollahi, R. A. Rahchamani, *J. Electroanal. Chem.*, 520(2002)145.
14. M.Rudolph, *J. Electroanal. Chem.*, 558(2003)71.
15. D. Nematollahi, S. M. Golabi, *J. Electroanal. Chem.*, 481 (2000) 208.
16. S. M.Golabi, F. Nourmohammadi, A.Saadnia, *J. Electroanal. Chem.*, 548(2003) 41.
17. D. Nematollahi, M.Bamzadeh, H. Shayani, *Chem. Pharm. Bu ll.*, 58(2010)23-26.
18. K.T. Finley, in: S. Patai, Z. Rappoport, *The Chemistry of Quinonoid Compounds*, vol. 2, John Wiley & Sons, New York, (1988).
19. Y.S. Xu, C.C. Zeng, X.M. Li, R.G. Zeng, *J. Chin. Chem.*, 24(2006)1086-1094.
20. B. Lewall, H. Putter, *Chemosphere*, 43 (2001)63–73.
21. R. Asami, M. Atobe, T. Fuchigami, *J. Am. Chem. Soc.*, 127(2005)13160–13161.
22. I. Tabakovic , Z. Grujic , Z. Bejtovic , *J. Heterocyc. Chem.*, 20 (1983)635–638.
23. D. Nematollahi, D. Habibi, M. Rahmati, M. Rafiee, *J. Org. Chem.*, 69(2004)2637–2640.

24. A.R. Fakhari, D. Nematollahi, M. Shamsipur, S. Makarem, S.S.H. Davarani, A. Alizadeh, H.R. Khavasi, *Tetrahedron*, 63(2007)3894–3898.
25. S.S.H. Davarani, D. Nematollahi, M. Shamsipur, N.M. Najahi, L. Masoumi, S. Ramyar, *J. Org. Chem.*, 71(2006)2139–2142.
26. D. Nematollahi, M. Alimoradi, S. Waqif Husain, *Electrochim. Acta.*, 51(2006)2620–2624.
27. D. Nematollahi, M.S. Workentin, E. Tammari, *Chem. Commun.* 15 (2006)1631–633.
28. R.H. Thomson, Naturally Occurring Quinones, Chapman and Hall, London, 4th ed., Academic Press, London, (1997).
29. P.R. Rich, *Faraday Discuss. Chem. Soc.*, 148(1982) 54.
30. H.S. Sutherland, K.C. Higgs, N.J. Taylor, R. Rodrigo, *Tetrahedron*, 57(2001)309.
31. G. Bringmann, S. Tasler, *Tetrahedron*, 57(2001)331.
32. V.S. Nithianandam, S. Erhan, *Polymer*, 32(1971)1146.
33. K. Kaleem, F. Chertok, S. Erhan, *Prog. Org. Coat.*, 15(1987)63.
34. M. Rafiee, D. Nematollahi, *Electrochim. Acta.*, 53(2008)2751.
35. H. Jaegfeldt, A.B.C. Torstensson, L.G.O. Gorton, G. Johansson, *Anal. Chem.*, 53 (1981)1979.
36. Afkhami, D. Nematollahi, T. Madrakian, L. Khalafi, *Electrochim. Acta.*, 50(2005) 5633.
37. D. Nematollahi, D. Habibi, M. Rahmati, M. Rafiee, *J. Org. Chem.*, 69(2004)2637.
38. M. Rafiee, D. Nematollahi, *J. Electroanal. Chem.*, 626(2009)36.
39. D. Nematollahia, M. Rafieeb and L. Fotouhic, *J. Iran. Chem. Soc.*, 6(2009)448-476
40. H. Jaegfeldt, A.B.C. Torstensson, L.G.O. Gorton, G. Johansson, *Anal. Chem.*, 53(1981)1979.
41. L. Fotouhi, M. Mosavi, M.M. Heravi, D. Nematollahi, *Tetrahedron*, 62(2006) 8553.
42. L. Fotouhi, D. Nematollahi, M.M. Heravi, E. Tammari, *Tetrahedron*, 47(2006) 1713.
43. L. Fotouhi, M. Zeienali, S. Dehghanpour, D. Nematollahi, *J. Chin. Chem.*, 25 (2007)1.
44. L. Fotouhi, D. Nematollahi, M.M. Heravi, *J. Chin. Chem. Soc.*, 54(2007)1163.
45. D. Nematollahi, H. Goodarzi, *J. Org. Chem.*, 67(2002)5036.
46. D. Nematollahi, Z. Forooghi, *Tetrahedron*, 58(2002)4949-4953.

47. M. Shamsipur, S.S.H. Davarani, M. N.Aghdam, D.Nematollahi, *Electrochim. Acta.*, 51(2006)3327.
48. D. Nematollahi, E. Tammari, *J. Org. Chem.*, 70(2005)7769.
49. S.S.H. Davarani, D. Nematollahi, M. Shamsipur, *Heteroatom. Chem.*, 18(2007) 644.
50. J.B.Raof, R.Ojani, D.Nematollahi, A. Kiani, *Int. J. Elecochem.Sci.*, 4(2009)810-819.
51. D. Nematollahi, H. S. Jam, *Electrochim. Acta.*, 51(2006)6384.
52. M.M. Khodaei, A. Alizadeh, N. Pakravan, *J. Org.Chem.*, 73(2008)2527.
53. A.R. Fakhari, S.S.H. Davarani, H. Ahmar, S. Makarem, *J. Appl. Electrochem.*, 38(2008)1743.
54. F.J. Liu, C.C. Zeng, D.W. Ping, Y.L. Cai, R.G. Zhong, *J. Chin. Chem.*, 26(2008) 1651.
55. L.Fotouhi, S.Asadi, E.Tammari, M.M. Heravi, D.Nematollahi, *J. Iran. Chem. Soc.*, 5(2008)712-717.
56. C.C. Zeng, D.W. Ping, S.C. Zhang, R.G. Zhong, J.Y.Becker, *J. Electroanal. Chem.*, 622(2008)90.
57. X.Huang, R.Xu, M.D. Hawley, K.J.Kramer, *Biorg.chem.*, 25(1997)179-202.
58. H.J. Schafer, *Encyclopedia of Electrochemistry*, Vol. 8, *Organic Electrochemistry*, Wiley-VCH, Weinheim, (2004).
59. D.T. Sawyer, A.Sobkowiak, J.L. Roberts, *Electrochemistry for chemist*, 2nd ed., John Wiley and Sons, Inc., New work, (1995).
60. Southampton Electrochemistry group, *Instrumental methods in electro chemistry*, Horwood publishing Chichester, (2004).
61. A. J. Bard, L. R. Faulkner, *Fundamentals and Applications*, 2nd ed., John Wiley and Sons, Inc., New work, (2001).
62. J.B.Raof, R.Ojani, D.Nematollahi, A.Kiani, *J. Electrochem.Sci.*, 4(2009)810-819.
63. D. Nematollahi, R.A. Rahchamani, *J. Electroanal.Chem.*, 520(2002)145.
64. D. Nematollahi, R.A. Rahchamani, *J. Electroanal.Chem.*, 520(2002)145.
65. A. K. Timbola, Cristine, D. de Souza, C. Giacomelli, A. Spinelli, *J. Braz. Chem. Soc.*, 17 (2006)139-148.
66. L. Fotouhi, M. Khakpour, D. Nematollahi, M.M. Heravi, *ARKIVOC* (ii)(2008)43-52.
67. S.A.M. Refaey, A.A. Hassan, H.S. Shehata, *J. Electrochem. Sci.*, 3(2008)325 -337.

68. L. Papouchado, G. Petrie, J.H. Sharp, R.N. Adams, *J. Am. Chem. Soc.*, **90** (1968)5620–5621.
69. S.S.H. Davarani, D. Nematollahi, M. Shamsipur, N.M. Najahi, L. Masoumi, S.Ramyar, *J. Org. Chem.*, **71**(2006)2139–2142.
70. R.S. Nicholson and I. Shain, *Anal.chem.*, **38**(1966)1406.